Atomic and Molecular Processes in Plasma Decomposition Method of Hydrocarbon Gas*)

Makoto OYA, Ryosuke IKEDA[1)] and Kazunari KATAYAMA

Faculty of Engineering Science, Kyushu University, Fukuoka 816-8580, Japan

[1)]*Interdisciplinary Graduate School of Engineering Sciences, Kyushu University, Fukuoka 816-8580, Japan*

(Received 28 November 2019 / Accepted 19 March 2020)

In order to understand the decomposition process of hydrocarbons in a hydrogen (H) plasma, a Monte Carlo simulation of collisional transport of a methane (CH_4) molecule was developed. The model simulates collision reactions with plasma ions and electrons (including dissociation, excitation, ionization, and charge exchange) and elastic collisions with residual H_2 gas. The interaction with a surrounding wall was also considered (reflection from the wall, deposition on the wall, and reemission of carbon (C) and hydrocarbons (CH_x) by physical and chemical sputtering). In a low-temperature plasma, because the decomposition process was mainly dominated by charge exchange with plasma ions followed by dissociative recombination with electrons, many neutral C and CH_x species were obtained. At high temperature, the ionized C^{y+} and CH_x^+ species were the dominant ones because of the dissociative ionization and excitation by electrons. Comparable to our previous experiment, the calculated decomposition rate of CH_4 into neutral and ionized C atoms was ~50% for a temperature of 15 eV and a density of 3.5×10^{17} m^{-3}. Nevertheless, the calculated distribution of C and CH_x deposits on the vessel wall were localized in the upstream of the plasma, which was different from the experimental setup.

Keywords: fusion reactor, hydrogen isotope recovery, hydrocarbon, plasma decomposition method, Monte Carlo simulation, ionization, dissociation, elastic collision, reflection, sputtering

DOI: 10.1585/pfr.15.2405032

1. Introduction

Hydrogen isotope recovery from vacuum exhaust gas is an essential method in ensuring the safety of tritium and efficiency of fuel cycle in a fusion reactor. Even in full-metal wall devices, the vacuum exhaust gas can contain hydrocarbons because carbon (C) atoms dissolve in the metals (tungsten and steel) and are deposited on the metal surfaces, as shown in QUEST at Kyushu University [1]. Therefore, through decomposition of the hydrocarbons, hydrogen isotopes have to be recovered.

We have introduced a new method of hydrocarbon decomposition using plasma and evaluated it experimentally. In the experiments [2, 3], methane (CH_4) gas was injected into a radio-frequency (RF) plasma. The results presented that almost all CH_4 injected was decomposed into carbon (C) and hydrogen (H) atoms by a helium plasma. However, in the case of H plasma, the decomposition was limited to be less than 70%. Furthermore, C-based by-products were deposited on the inner wall of the plasma vessel, decreasing the H recover efficiency. To improve the recovery efficiency, the details of CH_4 decomposition and C deposition processes must be understood from the viewpoints of both atomic and molecular collisions in the plasma and plasma-wall interactions on the vessel wall.

In this study, we developed a Monte Carlo simulation of three-dimensional transport of CH_4 molecules in a cylindrical H plasma surrounded by a vessel wall. Our attention is focused on the case that a small amount of CH_4 gas is injected into a real-sized plasma with a thick C-deposited wall to simulate experimental setup in a steady-state condition.

2. Simulation Model

As in the experimental setup [3], a quartz vessel with a length d of 27 cm and a radius r of 0.5 cm surrounded a cylindrical H plasma. Figure 1 (a) presents the axial distribution of the electron density n_e and temperature T_e of the plasma used in this simulation. The radial distribution of the plasma parameters was disregarded. The ion temperature T_i was assumed to be equal to T_e. A H_2 gas was introduced into the vessel to produce the plasma. The gas pressure was set to 170 Pa, which corresponds to a density of H_2 neutrals of 4.1×10^{22} m^{-3}. A double-probe method in the previous study [4] experimentally measured the electron temperature and density in this plasma. The measurement results showed $n_e = 6.7 \times 10^{16}$ m^{-3} and $T_e = 9.25$ eV at the axial position of $d = +11.5$ cm [+6.0 cm away from the edge of plasma center ($d = +5.5$ cm)]. To estimate the axial distribution of n_e, optical spectroscopy was conducted at other three points ($d = +7.5, +9.5, +10.5$ cm). From the relative ratio of emission strength, n_e were es-

author's e-mail: moya@aees.kyushu-u.ac.jp

*) This article is based on the presentation at the 28th International Toki Conference on Plasma and Fusion Research (ITC28).

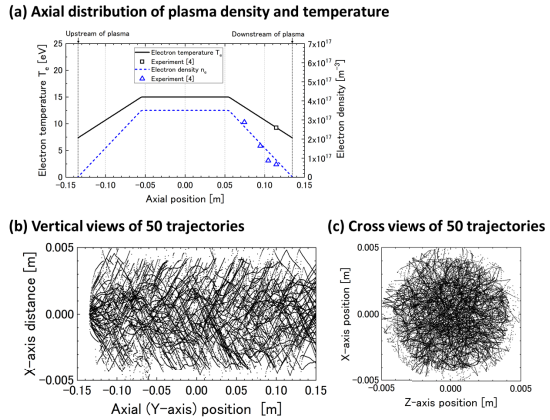

Fig. 1 (a) Axial distributions of plasma density n_e and temperature T_e used for simulation. (b) Vertical and (c) cross views of 50 pseudo-particles of CH_4 molecules injected from the position of $d = -13.5$ cm on the center axis of a cylindrical vessel.

timated to be 2.9×10^{17} m^{-3} at +7.5 cm, 1.6×10^{17} m^{-3} at +9.5 cm, and 8.7×10^{16} m^{-3} at +10.5 cm. Based on these experimental evidences, at the plasma center region, n_e were estimated to be 3.5×10^{17} m^{-3} by extrapolating four results (one probe data and three emission data), and the axial distribution was estimated as shown in Fig. 1 (a). On the other hand, we have only one data on T_e (9.25 eV at $d = +11.5$ cm). The effect of T_e axial distribution is discussed in Section 3.

In this simulation, CH_4 molecules (typically, the number of 10^3) were injected into the plasma edge ($d = -13.5$ cm) and the center of axis ($r = 0.0$ cm). Each molecule was assumed to be a pseudo-particle representing the number of 3.62×10^{17} CH_4 molecules per second. The initial velocity distribution of the pseudo-particle was a Maxwellian in a temperature of 300 K, shifted by the flow velocity of 0.025 m s^{-1} (approximately corresponding to the CH_4 gas flow introduced from a 1/8-inch pipe). In addition, by vacuum pumping at the end of the vessel, a superficial velocity of 38.2 m s^{-1} pushed the particles along the cylindrical axis at all times.

The pseudo-particle that move across the plasma experienced many collision types with plasma particles and also residual neutrals. In the case of plasma particles (ions and electrons), the 89 types of collision reactions were followed using the atomic data package from ref. [5], i.e., the direct ionization, dissociative ionization, excitation of hydrocarbon ions, dissociative recombination of the ionized particles, and charge exchange with the H^+ ions. The reaction sequences generated many species of hydrocarbon neutrals CH_x ($x = 1$ - 3) and the ions CH_x^+ ($x = 1$ - 4), finally resulting in neutral and ionized C^{y+} ($y = 0$ - 6). On the other hand, in the case of residual neutrals (H_2), the pseudo-particles collided with H_2 elastically. The scattering angle and energy loss in this elastic collision were simply calculated assuming hard-sphere collision [6].

When the pseudo-particles reached the vessel wall ($r = 0.5$ cm), they are reflected or deposited on the wall. The ionized species CH_x^+ ($x = 1$ - 4) are accelerated by the electric field in the electrostatic sheath before bombarding the wall surface. The sheath thickness was set to be 16.3 λ_D, where λ_D is the Debye length, and the electric field was calculated according to ref. [7]. A part of the particles reaching the wall surface was reflected and moved back into the plasma, and they collided again with the plasma particles (electrons and ions) and neutrals. The reflection coefficient depends on the species and energy of the molecules. Moreover, different species are emitted from the wall surface when they are reflected. This emission probabilities of each species were taken from a molecular dynamics simulation from ref. [8] at relevant incident energies. The wall surface was assumed to be a C-deposited layer, which was too thick to be penetrated by the incident particles, and an amorphous C including rich H atoms (atomic ratio H/(C + H) of 0.3) because of successive bombardment of plasma H ions. The charging effects on the quartz vessel wall were not taken into account because of the thick conducting layer. From the surface, low-energy (< 10 eV) and large molecules are easy to reflect as they are, whereas with increasing energy, the molecules are decomposed into small species and C atoms. The CH_x molecules and C atoms that were not reflected from the surface were deposited on the wall. They are a subject to physical and chemical sputtering because of successive irradiation with plasma H^+ ions. Therefore, the number of deposited C atoms and CH_x molecules in a pseudo-particle was calculated by subtracting the number of sputtered particles. In this simulation, the sputtering yield was calculated using a semi-empirical formula for pure C material from ref. [9] with a target temperature of 450 K taken from the experiment. In the experiment [3], the wall temperature decreased to 300 K toward the edges of this devise ($d < -15$ cm and $d > +15$ cm). The temperature distribution was not taken into account because it did not affect sputtering yield strongly at this temperature region. The chemical or physical sputtering was chosen based on each sputtering yield. For chemical sputtering, a CH_4 molecule with a Maxwellian-distributed velocity with the wall temperature was reemitted from the surface, whereas for physical sputtering, a C atom with Thompson energy distribution was emitted. The calculation finished when pseudo-particles reached the axial edges of this devise ($d < -15$ cm and $d > +15$ cm). They were assumed to be transported without deposition and reflection. Nevertheless, small part (~0.1%) of CH_x molecules escaped from the axial edges in the experimental condition ($T_e = 15$ eV and $n_e = 3.5 \times 10^{17}$ m^{-3}).

Figures 1 (b) and (c) shows vertical and cross pictures, respectively, of 50 pseudo-particles of an injected CH_4 molecule moving in the plasma, decomposing into small molecules and atoms. In the vertical picture, the axial scale is reduced to 1/15. Every 10^{-6} s, each point is sketched by

the positions of the pseudo-particles. The number of points reduced near the vessel wall surface because an ionized particle was accelerated by the sheath electric field.

3. Simulation Results

First, the effect of T_e axial distribution on simulation results was examined. The calculations were conducted using trapezoid- and flat-type distributions as shown in Fig. 2. The results of the simulation and the distribution of species (C atoms and CH_x molecules) were shown in Fig. 2 (b). It can be seen from Fig. 2 (b) that the T_e axial distributions did not make large difference on particle distributions; therefore, the distribution found in Fig. 1 (a) is used hereafter.

Figure 3 presents the distributions of species deposited on the vessel wall or passed through the plasma. Plasma parameters were set to be the same with the experimental condition (T_e = 15 eV and $n_e = 3.5 \times 10^{17}$ m^{-3}) shown in Fig. 3 (b). For comparison, low T_e case (1 eV) and high T_e case (100 eV) are shown in Figs. 3 (a) and (c), respectively, with $n_e = 1 \times 10^{17}$ m^{-3}. The decomposition of the injected CH_4 was conducted in all cases [Figs. 3 (a) - (c)] but with different species distributions. In the low-temperature plasma [Fig. 3 (a)], neutral species were dominant, and a large part of neutrals escaped from the downstream of the plasma (axial position d around +0.135 m). For higher T_e [Fig. 3 (b)], the ionized species were mainly developed, and the decomposition was considered adequate to produce singly and multi-charged C ions. With the further increase of T_e [Fig. 3 (c)], CH_x^+ ions were dominant on the species distribution, therefore reducing the decompositions of C atom.

In order to understand the decomposition process of the injected CH_4 molecules, we assessed which collision reactions occurred in the above three cases. Figure 4 demonstrates the occurred collision reactions in this simulation, which are categorized into seven types. In low-temperature plasma [Fig. 4 (a)], C^+ and CH_x^+ ions were produced through a charge exchange reaction involving dissociations of CH_4 neutrals with plasma ions. The ions were neutralized under dissociative recombination with the electrons and also through reflection from the vessel wall, therefore, obtaining many neutral species, as shown in Fig. 3 (a). At the experimental condition case [Fig. 4 (b)], the dissociative ionization of CH_4 neutrals, the dissociation of CH_4 neutrals, and the dissociative excitation of the ionized products frequently occurred, resulting in single ionization of C atoms. Further increase in plasma temperature [Fig. 4 (c)] resulted in a reduction in the number of collision reactions since the ion species early deposited into the vessel wall.

The dependences of the plasma parameter (n_e and T_e) on the decomposition were also examined. The decomposition rate was defined to be a percent fraction of the

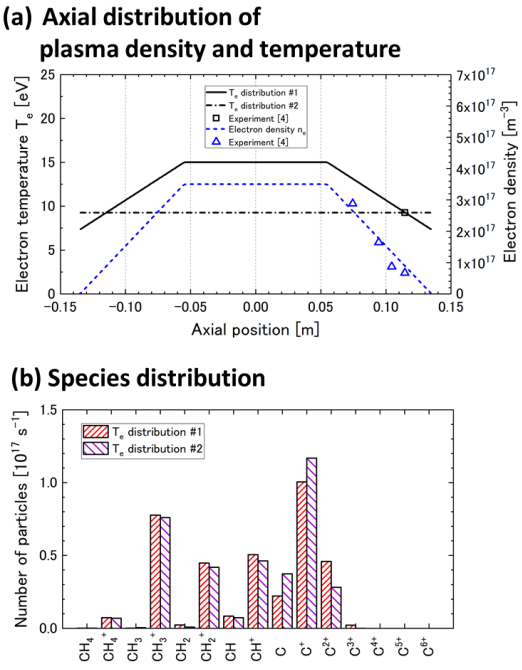

Fig. 2 (a) Axial distributions of plasma density n_e and temperature T_e used for simulation. (b) Species distribution after calculation.

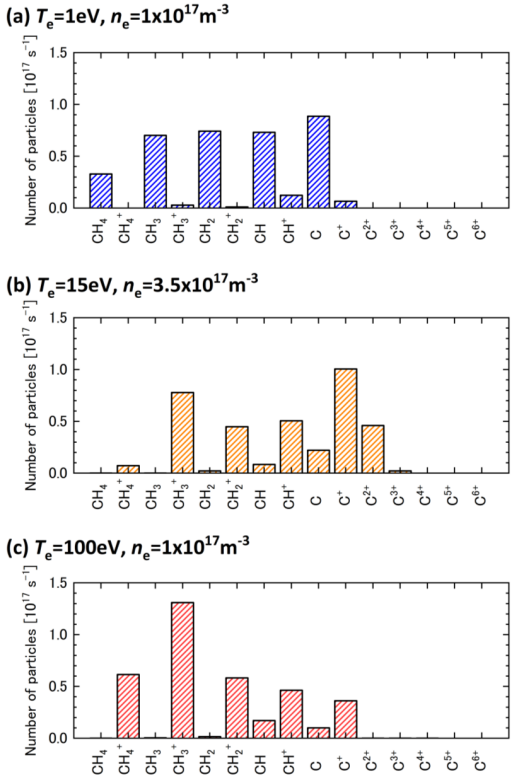

Fig. 3 C and CH_x species deposited on the vessel wall or escaped from the downstream of plasma with different temperatures, T_e, at the center of the plasma. (a) T_e = 1 eV ($n_e = 1 \times 10^{17}$ m^{-3}), (b) T_e = 15 eV ($n_e = 3.5 \times 10^{17}$ m^{-3}), and (c) T_e = 100 eV ($n_e = 1 \times 10^{17}$ m^{-3}). The number of injected CH4 molecules is 3.62×10^{17} per second.

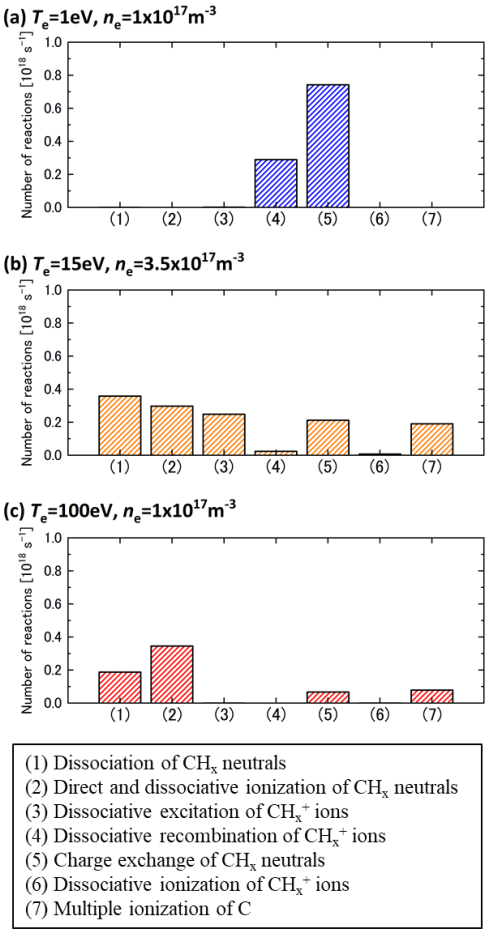

Fig. 4 Collisional reactions occurred in the vessel before the deposition on the vessel wall or escaped from the downstream of plasma. Plasma parameters in (a), (b), and (c) correspond to the cases in Figs. 3 (a), 3 (b), and 3 (c), respectively. The number of injected CH4 molecules is 3.62×10^{17} per second.

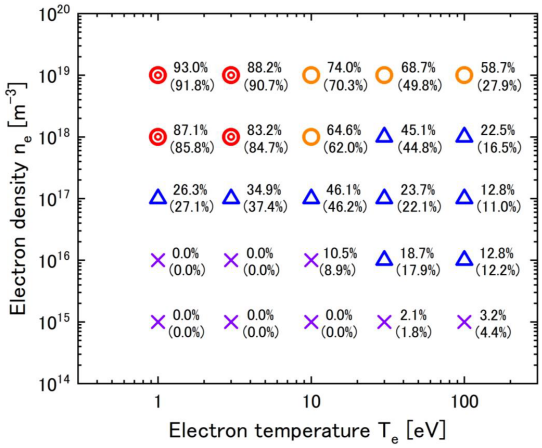

Fig. 5 Plasma parameter dependence of the decomposition rate that is defined as a percent fraction of neutral and ionized C atoms to the injected CH_4 molecules. The values inside the parentheses are the rates calculated without sputtering from and redeposition on the deposited C and CH_x. The double circle, circle, triangle, and cross symbols correspond to the rates, R_d, of $R_d > 80\%$, $80\% > R_d > 50\%$, $50\% > R_d > 10\%$, and $R_d < 10\%$, respectively.

number of fully dissociated C atoms (neutrals and ions) to injected CH_4 molecules. Figure 5 summarizes the calculation results where the decomposition rates were categorized using four symbols, i.e., double circle, circle, triangle, and cross with the value of the rate. The values in parentheses are the rates calculated without sputtering and redeposition of C and CH_x deposits. The calculation results showed that low-temperature and high-density plasma was desirable for high decomposition rate, regardless of whether the sputtering and redeposition were considered. For the decomposition rate of more than 60%, $n_e > 5 \times 10^{17}\,\mathrm{m}^{-3}$ and $T_e < 30\,\mathrm{eV}$ were needed. In high-density cases ($10^{18}\,\mathrm{m}^{-3}$ and $10^{19}\,\mathrm{m}^{-3}$), the decomposition rate decreased with increasing temperature. There were quite different dependences on the electron temperatures in the low- and high-plasma-density cases because at high temperatures, the ionized products were deposited after few dissociations due to the sheath acceleration before reaching the wall surface. Differently, there were increased collision events for the decomposition due to the increasing density of the plasma. In our experiments [3], an inductively coupled plasma was produced by the RF power of 50 W and the H_2 gas pressure of 170 Pa. The plasma parameters achieved in the experiments are estimated to be $n_e = 3\text{-}5 \times 10^{17}\,\mathrm{m}^{-3}$ and $T_e = 10\text{-}15\,\mathrm{eV}$ at the center axis in the cylindrical vessel. Therefore, the present simulation was in rough agreement with the experimental estimation value of 60% - 70%, although the decomposition rate was defined differently from the simulation. (In the experiment, the CH_4 signal was obtained by a quadrupole mass spectrometer equipped at the downstream of the plasma vessel. The ratio of the signals with-plasma to without-plasma was calculated.)

In the experiment [3], thick C and CH_x deposits were observed at the downstream of the plasma, and the deposits were strongly suppressed around the center of the plasma. This suppression of the deposition at the center region may be explained by the sputtering of the deposited C and CH_x. In this simulation, a pseudo-particle represented the number of 3.62×10^{17} of CH_4 molecules per second, which corresponds to a flow rate of 0.81 sccm (standard cubic centimeters per minute) in the experiment. Therefore, the axial distribution of deposited C and CH_x can be assessed for the experimental conditions. Figure 6 presents the axial distributions for different electron temperatures T_e. High T_e [Fig. 6 (c)] produced a localized and thick deposition in the upstream of the plasma (axial position d around -0.135 m). With decreasing T_e, the deposition became thinner and was distributed in a wider area of the vessel. In the experimental condition [Fig. 6 (b)], the distributions are shown together with calculation without

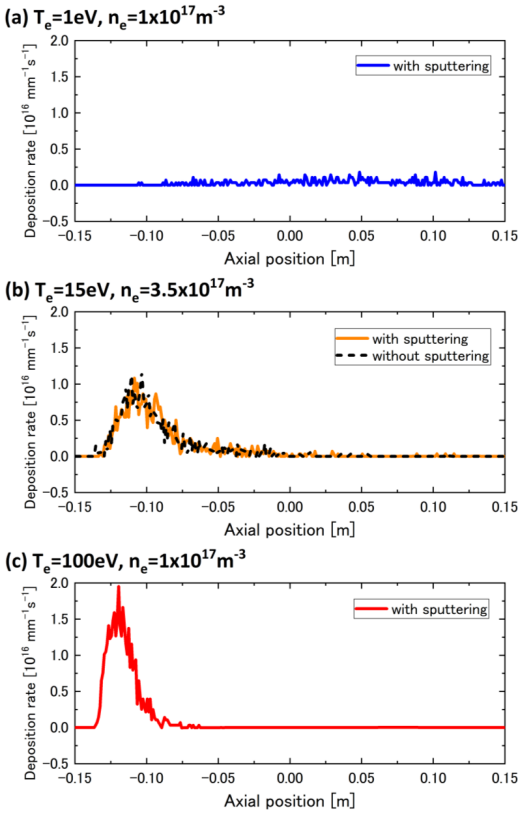

Fig. 6 Axial distribution of C and CH_x deposits on the vessel wall for different temperatures T_e at the center of the plasma. Plasma parameters in (a), (b), and (c) correspond to the cases in Figs. 3 (a), 3 (b), and 3 (c), respectively. The number of injected CH_4 molecules is 3.62×10^{17} per second. The distribution calculated without sputtering and redeposition effects on C and CH_4 deposits due to plasma ion bombardment is shown in figure (b), represented with dotted line.

sputtering of the deposits (C atoms and CH_4 molecules) by plasma H ions. Regardless of whether the sputtering from the deposited C on the wall was considered or not, the deposition was distributed to the upstream of the plasma. The distribution was somewhat different from the experimental results where distribution had a peak at the downstream of the plasma. The sputtering yield, which was calculated using a semi-empirical formula [9], was 0.0068 at the center position. Such a small yield caused few sputtering in the plasma cylinder within the length of 27 cm, e.g., one CH_4 molecule (not pseudo-particle) experienced ~1 time sputtering for $n_e = 3.5 \times 10^{17}$ m^{-3} and $T_e = 15$ eV. The reason for the disagreement with the experimental observation was unclear. Although the empirical sputtering yield of pure C utilized here was insensitive to the target temperature for the temperatures < 500 K, the axial profile of the C and CH_x deposits observed in the experiment strongly correlated with the wall temperature. Most deposits were observed at the axial edge of the vessel where there was relatively low wall temperature. One possibility of the temperature-dependent deposition may be a result of containing H atoms in the deposited C, producing, for example, a-C:H. The H uptake increases the sputtering yield of loosely bound C from thick a-C:H layer with elevated surface temperatures at low energies of incident H in the range of 1 - 10 eV [10]. Furthermore, to improve the erosion of the deposits, the charge exchange reaction of plasma H ions with neutral H atoms emitted by CH_4 decomposition can produce high-energy H atoms. Tentative simulation calculations were performed by using higher sputtering yields that were 10 and 100 times higher than the semi-empirical yield. Figure 7 presents the calculation results that cause us to expect the growth of the additional peak at the downstream of the plasma. For the highest sputtering yield, strong erosion in the upstream of the plasma was obtained, and the eroded deposits were redeposited at the downstream of the plasma.

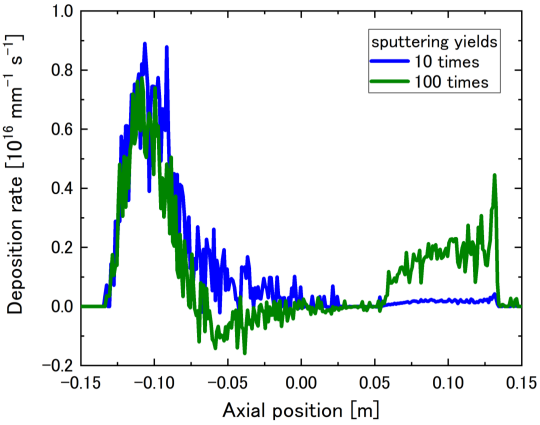

Fig. 7 Tentative calculation of the axial distribution of C and CH_x deposits on the vessel wall for high sputtering yields. The sputtering yields are 10 and 100 times higher than the semiempirical yield [9]. Plasma density and temperature are 3.5×10^{17} m^{-3} and 15 eV, respectively. The number of injected CH_4 molecules is 3.62×10^{17} per second.

Here, the effect of neutral H atoms emitted by CH_4 decomposition on sputtering is discussed. high-energy H atoms may be produced through charge exchange reaction of plasma H ions with the neutral H atoms. The number of the emitted H atoms bombarding the vessel wall had peaked to $\sim 2.5 \times 10^{16}$ per second (within an interval of 1 mm of the axial position) at the upstream of the plasma ($d \approx -0.1$ m). It is smaller than the number of plasma H ions ($\sim 1 \times 10^{17}$ per second) bombarding the vessel wall. The effect of the sputtering by the H atoms emitted by CH_4 decomposition on the deposition profile can be small because the sputtering yield was less than 0.01 even for the energy of 100 eV. In addition, the effect of the sputtering by C and CH_x products is also discussed. An impact of C and CH_x (including C dissociated from CH_x at the surface) mainly causes self-sputtering of the deposits. The sputtering yield is 0.01 or less even at the center region of the plasma ($d = -0.55$ - $+0.55$ m) because the threshold energy for the self-sputtering is high (30 eV or more) [11].

Therefore, the effect of the self-sputtering of the C and CH_x deposits can be small again. Contrarily, the sputtering by impurities in the plasma, such as multiply ionized C and O, gives us another possibility to explain the difference of deposition profile between experiment and simulation results. Assuming that a concentration of C^{3+} impurities was several %, the number of the impurity ions bombarding the vessel surface is less than 10^{16} per second (with an interval of 1 mm at the axial position). The sputtering yield by the ions accelerated in the plasma sheath is ~0.12 even at the center region of the plasma. This gives us a small contribution of plasma impurities to the deposition profile [Fig. 6 (b)].

4. Conclusion

A Monte Carlo simulation of a CH_4 molecule collisional transport in H plasma with residual H_2 gas was employed to evaluate the decomposition process with various plasma parameters. In the simulation, surface processes were also taken into account, namely, reflection of C and CH_x products, deposition on a cylindrical vessel wall, and sputtering of the deposits. Since the decomposition process was dominated by a reaction chain of the charge exchange with plasma ions and dissociative recombination with electrons, many neutral C and CH_x species were obtained in low-temperature plasma. With increasing temperature, the ionized species mainly dominated the decomposition products due to dissociation and dissociative ionization of CH_x neutrals and dissociative excitation of CH_x^+ ions. The ion species were easier (harder) to deposit into (reflected from) the wall surface because of the sheath acceleration before reaching the wall surface. As a result, the decomposition of CH_4 molecules was gradually suppressed with increasing temperature at high densities, whereas with increasing density of the plasma, it was largely enhanced. The calculated decomposition rate of CH_4 into neutral and ionized C atoms was ~50% for a density of 3.5×10^{17} m^{-3} and a temperature of 15 eV, which was comparable to an estimation in our previous experiment. Nevertheless, the calculated distributions of the C and CH_x deposits to the vessel wall were localized in the upstream of the plasma, and additional deposition at the downstream of the plasma is not reproduced by this simulation.

Acknowledgment

The author thanks Dr. K. Ohya for his encouragement with simulation code development and discussion. This work was supported by the Grant-in-Aid for Scientific Research of MEXT KAKENHI (17H06934, 18K13527).

[1] Z. Wang *et al.*, Rev. Sci. Instrum. **88**, 093501 (2017).
[2] K. Katayama *et al.*, Fusion Eng. Des. **82**, 1381 (2010).
[3] S. Kasahara, Fusion Sci. Technol. **60**, 1487 (2011).
[4] S. Kasahara, Master thesis, Kyushu University, 2011, unpublished.
[5] R.K. Janev and D. Reiter, Rep. Forshungszentrum Julich, Jul-3966 (2002).
[6] T. Motohiro and Y. Taga, Thin Solid Films **112**, 161 (1984).
[7] K. Shiraishi and S. Takamura, J. Nucl. Mater. **176&177**, 251 (1990).
[8] K. Ohya, AIP Conf. Proc. **1237**, 47 (2010).
[9] J. Roth, J. Nucl. Mater. **266-269**, 51 (1999).
[10] K. Ohya *et al.*, 2010 Fusion Energy Conference, IAEA, THD/P3-04.
[11] W. Eckstein *et al.*, Rep. Max-Planck-Institut für Plasmaphysik, IPP 9/82, 1993.